

Impact of the masonry infills on the correlation between seismic intensity measures and damage of R/C buildings

Konstantinos G. Kostinakis*

Department of Civil Engineering, Aristotle University of Thessaloniki, Aristotle University Campus, 54124, Thessaloniki, Greece

(Received December 15, 2017, Revised January 24, 2018, Accepted January 25, 2018)

Abstract. This paper investigates the role of the masonry infills on the correlation between widely used earthquake Intensity Measures (IMs) and the damage state of 3D R/C buildings taking into account the orientation of the seismic input. For the purposes of the investigation an extensive parametric study is conducted using 60 R/C buildings with different heights, structural systems and masonry infills' distributions. The results reveal that the correlation between the IMs and the seismic damage can be strongly affected by the masonry infills' distribution, depending on the special characteristics of the structural system, the number of stories and the incident angle.

Keywords: reinforced concrete; masonry infills; nonlinear dynamic analysis; seismic excitation angle; seismic damage; ground motion intensity measures; correlation between IMs and seismic damage

1. Introduction

Performance-Based Earthquake Engineering (PBEE) (Cornell and Krawinkler 2000), which aims at the quantification of the damage risk and seismic performance of structures due to future earthquakes, has received considerable attention during the past years. When PBEE is applied, the seismic performance is usually computed via nonlinear time history analysis of the examined structures for strong motions that are consistent with the hazard at the building site (Jayaram *et al.* 2010). In the context of this analysis method many provisions about the nonlinear behavior of Reinforced Concrete (R/C) structures are provided by the seismic codes. However, the code provisions do not consider, amongst others, the role of the masonry infills on the structural response, which is addressed by the seismic codes only by general instructions.

Reinforced Concrete (R/C) structures with unreinforced masonry infills are amongst the most common structural systems for low- and medium-rise buildings in many countries with regions of high seismicity. The observation of post-earthquake damages on R/C structures has led to the conclusion that the presence of masonry infills may significantly alter the seismic performance of the buildings (e.g., EERI 2000, Ricci *et al.* 2010). More specifically, experimental and numerical researches have shown that a uniform distribution of masonry infill walls can lead to the increase of lateral stiffness and robustness, thus modifying the dynamic characteristics of the building, resulting in a lower period of vibration (e.g., Bertero and Brokken 1983, Ricci *et al.* 2011). On the other hand, if the infill walls are unevenly distributed, negative effects may be induced, such

as the soft story mechanism. This phenomenon is caused when the first story is left open for architectural reasons, while the upper stories are infilled with masonry walls (pilotis). In this case, severe localized damage or collapse of the first story can be caused during a strong earthquake (e.g., Negro and Colombo 1997, Das and Nau 2003).

The influence of the masonry infills on the nonlinear response of R/C buildings can be crucial, as it has been shown by numerous studies. For example, Dolsek and Fajfar (2008a, b) examined the effect of masonry infills on the seismic response of a four-story R/C concrete frame and revealed that the infills can completely change the distribution of damage throughout the structure, leading to beneficial effects when they are placed regularly. Later, Ricci *et al.* (2013) conducted a numerical investigation on the influence of infills on the seismic behavior of four different case study buildings. Another investigation was carried out by Mondal and Tesfamariam (2014), who conducted nonlinear static analyses of a six-story R/C frame in order to quantify the effects of vertical irregularity and thickness of masonry infills on the robustness of structures. They found that these infills' properties have significant influence on the response of the R/C building. More recently, Yuen and Kuang (2015) examined the seismic response and failure mechanisms of infilled R/C framed buildings with five different infill configurations. The analyses revealed that the degree of irregularity of the infill panels significantly affect the seismic performance of buildings, leading to more serious seismic damages.

During the process of the PBEE the expected damage caused by earthquakes of different intensities must be estimated. In order to estimate the structural damage potential of an earthquake it is necessary to introduce two intermediate variables, one describing the structural performance and the other describing the ground motion intensity. A successful correlation of the aforementioned

*Corresponding author, Post-Doctoral Researcher
E-mail: kkostina@civil.auth.gr

variables ensures more accurate evaluation of seismic performance and a sufficient reduction in the variability of structural response prediction. Consequently, the identification of an optimal Intensity Measure (IM), which sufficiently correlates with an appropriate Engineering Demand Parameter (EDP), is of great importance.

Several simple-to-elaborate conventional IMs that can be determined directly from the recorded earthquake time history have been used to estimate the damage potential of ground motions. Elenas (1997, 2000), Elenas and Meskouris (2001) studied the interdependency between several seismic acceleration parameters and the damage state of a 6-story (Elenas 1997) as well as an 8-story (Elenas 2000, Elenas and Meskouris 2001) planar R/C frame structure. They observed that for the structures under consideration spectral and energy-related seismic intensity measures correlate well with seismic damage. Liao *et al.* (2001), based on limited analyses of planar frames (5-story and 12-story R/C buildings), demonstrated that three parameters of the near-fault earthquake records, i.e., the ratio PGV/PGA, the spectral velocity and the input energy, are well correlated with the maximum story drift of the structures. Yakut and Yilmaz (2008) investigated the correlation between maximum interstory drift demand of 16 planar R/C frame structures and a number of widely used ground motion intensity measures. The results of this study demonstrated that spectrum intensity parameters have the strongest correlation. In order to examine the adequacy of seismic intensity measures to describe the structural response of R/C buildings under bidirectional strong motions, Cantagallo *et al.* (2012) investigated correlations between maximum interstory drift demand of nine 3D structures and a number of IMs. In this study, however, the two horizontal components of the earthquake records were applied along the structural axes of the buildings, thus the uncertainty introduced in the structural response by the seismic excitation angle is ignored. In another study, Kostinakis *et al.* (2015a) examined the correlation between a number of widely used ground motion intensity measures and the damage state of medium-rise 3D R/C buildings taking into account the orientation of the seismic input. The results revealed that the spectral acceleration at the fundamental period of the structure shows the strongest correlation with maximum and average interstory drift, followed by the velocity related seismic intensity measures.

It must be mentioned that all the above investigations were restricted to bare structures, thus ignoring the role of masonry infills on the results. To the best of the author's knowledge there is no study that has investigated the correlation between the seismic damage of infilled 3D R/C buildings and earthquake intensity measures. In a preliminary research work, Masi *et al.* (2011) correlated various measures of seismic intensity with the maximum interstory drift of typical 4-story R/C frames taking into account the influence of the masonry infills. They found that the Housner intensity is the IM that best correlates with the maximum interstory drift for the strong ground motions used in the study. However, in this study the correlation between a limited number of IMs and the damage state of only one planar building was examined. Furthermore, another critical issue that must be examined when

estimating the seismic response of 3-dimensional buildings is the influence of the incident angle on the inelastic response. As it has been shown by many researchers, even for buildings that are quite regular in-plan, the angle of seismic incidence can radically alter the analysis results in terms of the elastic response and design of structures (e.g., Athanatopoulou 2005, Kostinakis *et al.* 2012), as well as of the inelastic response and damage level (Rigato and Medina 2007, Lagaros 2010, Lucchini *et al.* 2011, Kostinakis *et al.* 2013, 2015b, Fontara *et al.* 2015).

The objective of the present paper is to investigate the correlation between the seismic damage of 3D infilled R/C buildings with various structural systems and a large number of widely used ground motion intensity measures, considering variable orientations of the earthquake ground motion. To accomplish this purpose an extensive parametric study is carried out. More specifically, 60 3-dimensional R/C buildings with different heights and structural systems are studied. The buildings are classified into three sets regarding the distribution of masonry infills: the first set contains 20 bare structures, the second set contains 20 structures with masonry infills in all the stories and the third set contains 20 structures with pilotis. The buildings are analyzed by means of Nonlinear Time History Analysis (NTHA) for 65 bidirectional strong motions. In order to account for the influence of the incident angle on the structural response, the two horizontal accelerograms of each ground motion are applied along horizontal orthogonal axes forming an angle $\theta=0^\circ, 5^\circ, 10^\circ, \dots, \dots, 355^\circ$ with the structural axes. For the evaluation of the inelastic structural behavior of each building the maximum interstory drift ratio is computed. Then, it is correlated with several strong motion intensity measures. The results reveal that the correlation between the examined IMs and the seismic damage is affected by the distribution of the masonry infills, depending on the choice of the IM, the special characteristics of the structural system and the number of stories. For each one of the three different distributions of the masonry infills, the research identified certain IMs that showed high correlation with the structural damage. Moreover, the influence of the masonry infills' distribution on the correlation coefficients is stronger in case of accounting for the angle of incidence. In this case, the correlation is stronger for the bare structures and weaker for infilled ones.

2. Ground motions

A suite of 65 pairs of horizontal bidirectional earthquake excitations obtained from the PEER (2003) and the European (2003) strong motion database was used as input ground motion for the analyses. The seismic excitations, which have been chosen from worldwide well-known sites with strong seismic activity, are recorded on Soil Type C according to EC8 (2003) and have magnitudes (M_s) between 5.5 and 7.8. The ground motion set employed was intended to cover a variety of conditions regarding tectonic environment, modified Mercalli intensity and closest distance to fault rupture, thus representing a wide range of intensities and frequency content. Another important aspect

considering the selection of the seismic excitations is that they provide a wide spectrum of structural damage, from negligible to severe, to the buildings investigated in the present study.

The horizontal recorded accelerograms of each ground motion were transformed to the corresponding uncorrelated ones rotating them about the vertical axis by the angle θ_o (Eq. (1)) (Penzien and Watabe 1975). Then, the pairs of the uncorrelated accelerograms have been used as seismic input for the analyses of the structures, as ASCE 41-06 (2008) proposes. The correlation factor of the recorded components ρ (Penzien and Watabe 1975) is given by Eq. (1)

$$\rho = \frac{\sigma_{xy}}{(\sigma_{xx} \cdot \sigma_{yy})^{1/2}}, \tan \theta_o = \frac{2\sigma_{xy}}{\sigma_{xx} - \sigma_{yy}} \quad (1)$$

with $\sigma_{ij} = \frac{1}{t_{tot}} \cdot \left(\int_0^{t_{tot}} \alpha_i(t) \cdot \alpha_j(t) dt \right)$ $i = x, y$

where $\alpha_x(t)$ and $\alpha_y(t)$ are the recorded ground accelerations along the two horizontal directions of the ground motion; σ_{xx} , σ_{yy} are the quadratic intensities of $\alpha_x(t)$ and $\alpha_y(t)$ respectively; σ_{xy} is the corresponding cross-term; t_{tot} is the duration of the motion.

3. Ground motion intensity measures

In order to define the intensity of the earthquake ground motion a large number of seismic intensity measures cited in the literature were considered in the present study. The definition as well as a discussion on the employment of each IM is presented in Kramer (1996). It must be noticed that many of the examined IMs have been widely used for correlation studies between seismic intensity and the damage state of planar structures (Elenas 2000, Elenas and Meskouris 2001, Liao *et al.* 2001, Yakut and Yilmaz 2008, Masi *et al.* 2011, Cantagallo *et al.* 2012, Kostinakis *et al.* 2015)

In particular, the following ground motion intensity measures are numerically assessed:

1. IMs determined from the time histories of the records
 - 1.1 Peak Ground Acceleration: $PGA = \max|a(t)|$
 - 1.2 Peak Ground Velocity: $PGV = \max|v(t)|$
 - 1.3 Peak Ground Displacement: $PGD = \max|d(t)|$
 - 1.4 Sustained Maximum Acceleration (SMA) is the 3rd largest peak in the acceleration time history
 - 1.5 Sustained Maximum Velocity (SMV) is the 3rd largest peak in the velocity time history
 - 1.6 Effective Design Acceleration (EDA) corresponds to the peak acceleration value that remains after filtering out accelerations above 9 Hz
 - 1.7 Root-Mean-Square (rms) of acceleration:

$$a_{rms} = \sqrt{\frac{1}{t_{tot}} \int_0^{t_{tot}} a(t)^2 dt}$$

- 1.8 Root-Mean-Square (rms) of velocity:

$$v_{rms} = \sqrt{\frac{1}{t_{tot}} \int_0^{t_{tot}} v(t)^2 dt}$$

- 1.9 Root-Mean-Square (rms) of displacement:

$$d_{rms} = \sqrt{\frac{1}{t_{tot}} \int_0^{t_{tot}} d(t)^2 dt}$$

- 1.10 Arias intensity: $I_a = \frac{\pi}{2g} \int_0^{t_{tot}} a(t)^2 dt$

- 1.11 Characteristic intensity: $I_c = (a_{rms})^{2/3} \sqrt{t_{tot}}$

- 1.12 Specific Energy Density: $SED = \int_0^{t_{tot}} v(t)^2 dt$

- 1.13 Cumulative Absolute Velocity:

$$CAV = \int_0^{t_{tot}} |a(t)| dt$$

2. IMs determined from the response spectra of the records

- 1.14 Acceleration Spectrum Intensity:

$$ASI = \int_{0.1}^{0.5} S_a(\xi = 0.05, T) dT$$

- 1.15 Velocity Spectrum Intensity:

$$VSI = \int_{0.1}^{2.5} S_v(\xi = 0.05, T) dT$$

- 1.16 Housner Intensity: $HI = \int_{0.1}^{2.5} PS_v(\xi = 0.05, T) dT$

- 1.17 Effective Peak Acceleration:

$$EPA = \frac{\text{mean}(S_a^{0.1-0.5}(\xi = 0.05))}{2.5}$$

where,

$a(t)$, $v(t)$ and $d(t)$: acceleration, velocity and displacement time history respectively

t_{tot} : total duration of ground motion

ξ : damping ratio

S_a, S_v : acceleration and velocity spectrum respectively

PS_v : pseudovelocity spectrum

The aforementioned IMs were determined for each one of the two components of the 65 bidirectional strong motions. However, in order to study the correlation of the IMs with the structural damage of the buildings, it was necessary to represent the intensity parameters corresponding to the two horizontal components by a single value. To achieve this, the Geometric Mean Value (GMV), which is the most widely used expression for the definition of horizontal bidirectional ground motion characteristics (Beyer and Bommer 2006) was used for each seismic excitation

$$IM_{GMV} = \sqrt{IM_1 \cdot IM_2} \quad (2)$$

where IM_1 and IM_2 : values of the IMs determined for each one of the two horizontal components of the ground motion. Three other alternative relations to express the IMs corresponding to the two horizontal components by a single value, that is the arithmetic mean value, the SRSS value and the maximum value over the two values, have been studied in Kostinakis *et al.* (2015a). In this study it has been proved that the variant relations to define a single IM corresponding

Table 1 Design data for all buildings

Name	Stories	Structural eccentricity e_0	Walls' Base shear along		Description of structural system
			axis x : n_{vx}	axis y : n_{vy}	
SFxy-3	3	0.0m	0.0%	0.0%	Symmetric Frame System along both axes x and y
SFxy-7	7	0.0m	0.0%	0.0%	
SWxy-3	3	0.0m	73.0%	76.0%	Symmetric Wall System along both axes x and y
SWxy-7	7	0.0m	65.0%	64.0%	
SFExy-3	3	0.0m	41.0%	41.0%	Symmetric Frame-Equivalent System along both axes x and y
SFExy-7	7	0.0m	43.0%	46.0%	
SFExFy-3	3	0.0m	43.0%	0.0%	Symmetric Frame-Equivalent System along axis x and Frame System along axis y
SFExFy-7	7	0.0m	38.0%	0.0%	
SWxHy-3	3	0.0m	77.0%	0.0%	Symmetric Wall System along axis x and Frame System along axis y
SWxHy-7	7	0.0m	66.0%	0.0%	
AFxy-3	3	0.98m	0.0%	0.0%	Asymmetric Frame System along both axes x and y
AFxy-7	7	2.39m	0.0%	0.0%	
AWxy-3	3	6.73m	66.0%	63.0%	Asymmetric Wall System along both axes x and y
AWxy-7	7	5.96m	65.0%	67.0%	
AFExy-3	3	4.65m	49.0%	46.0%	Asymmetric Frame-Equivalent System along both axes x and y
AFExy-7	7	3.79m	37.0%	36.0%	
AFExFy-3	3	2.23m	47.0%	0.0%	Asymmetric Frame-Equivalent System along axis x and Frame System along axis y
AFExFy-7	7	2.49m	35.0%	0.0%	
AWxHy-3	3	3.53m	67.0%	0.0%	Asymmetric Wall System along axis x and Frame System along axis y
AWxHy-7	7	3.01m	0.0%	65.0%	

to the two horizontal accelerograms produce almost the same correlation between IMs and damage measures.

4. Description, design and modeling of the nonlinear behavior of the selected buildings

For the purposes of the present investigation, ten double-symmetric (five 3-story and five 7-story) and ten asymmetric (five 3-story and five 7-story) in plan R/C buildings, with data supplied in Table 1 and Figs. 1 and 2 were studied. All buildings have structural system that consists of members in two perpendicular directions (axes x and y , Figs. 1 and 2). The names of the buildings investigated, along with the basic structural characteristics of each building, as well as the description of their structural system are given in Table 1 (the classification follows the classification of structural types of the EC8 (2003)). More specifically, the structural characteristics shown in this table are the number of stories, the structural eccentricity e_0 (where e_0 has been computed as the square root of e_{0x} and e_{0y}), as well as the fraction of the base shear forces along x - and y -axis that are received by the walls (if they exist).

For each one of the 20 buildings three different assumptions regarding the distribution of the masonry infills were adopted: (a) no masonry infills are present (bare structure), (b) masonry infills are uniformly distributed along the height (infilled structure) and (c) first story is bare and upper stories are infilled (structure with pilotis). It must be noticed that the seismic response of the buildings having the same structural system, but different distribution of

masonry infills can be completely different, since the existence of the masonry can significantly alter the building's structural response. Consequently, the total number of structures investigated in the present study is 20 different structural systems \times 3 different distributions of masonry infills=60.

All the above buildings were chosen so as to represent a large amount of R/C buildings designed with the aid of modern seismic codes. It must also be noted that in order to investigate the influence of the structural eccentricity on the results, the choice of the asymmetric buildings is made bearing in mind that their structural systems must be corresponding to those of the double-symmetric ones (Figs. 1 and 2). All buildings are regular in elevation according to the criteria set by EC8 (Paragraph 4.2.3.3). Also, for the asymmetric in plan buildings the distance between the mass centre and the stiffness centre, which defines the structural eccentricity e_0 , fulfils one of the following inequalities: $e_{0x} > 0.30r_x$ or $e_{0y} > 0.30r_y$. Therefore, these buildings display a high degree of asymmetry and can be classified as irregular in plan buildings (EC8, Paragraph 4.2.3.2). The symmetric buildings are regular in plan. In Table 2 all the common design data of the examined buildings are presented.

For the buildings' modeling all basic recommendations of EC8 (Paragraph 4.3.1), such as the diaphragmatic behavior of the slabs, the rigid zones in the joint regions of beams/columns and beams/walls and the values of flexural and shear stiffness corresponding to cracked R/C elements were taken into consideration. All buildings were considered to be fully fixed to the ground. Using the data given in Table 2, the upper limit values of the behavior

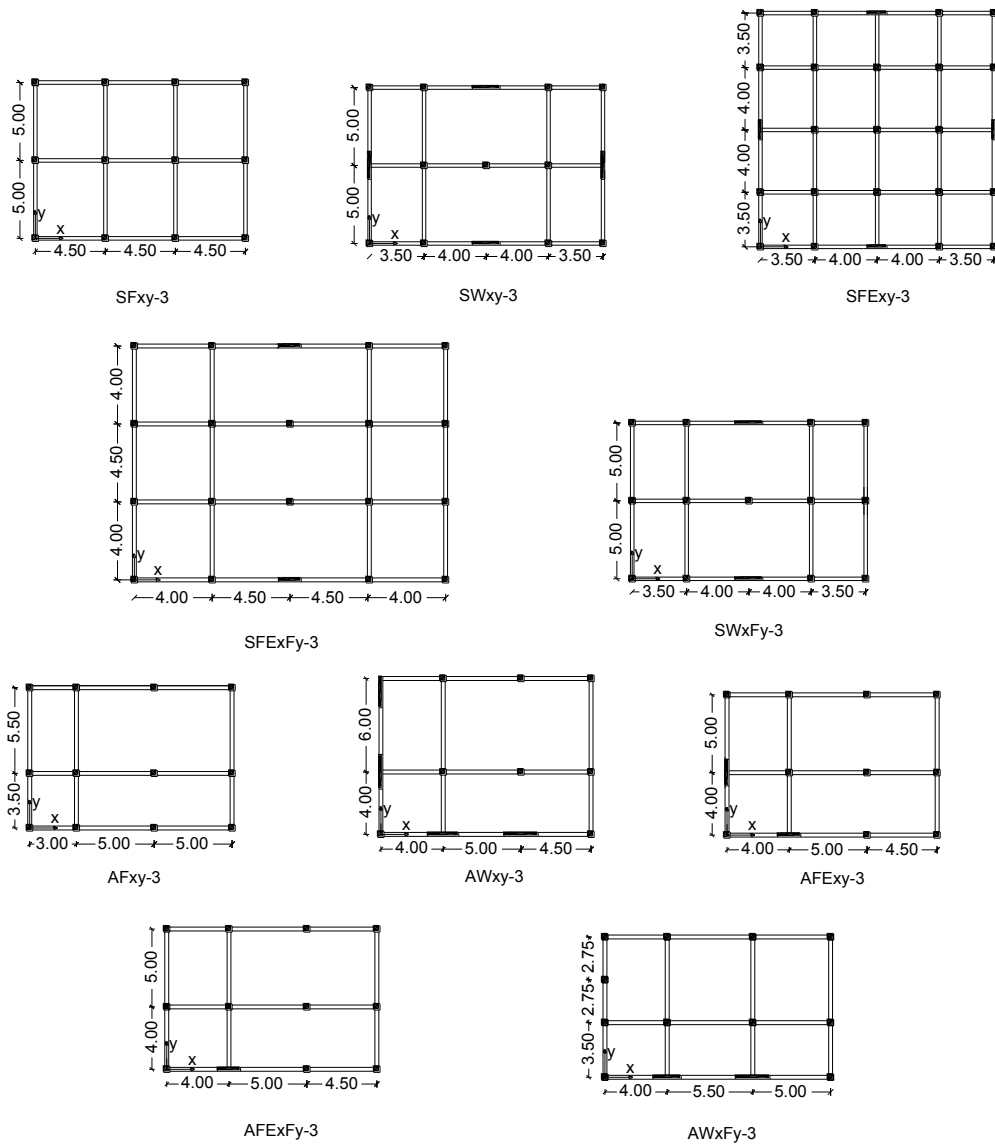


Fig. 1 Plan-views of the selected 3-story buildings

factor q according to EC8 (Paragraph 5.2.2.2) were determined.

The buildings were designed for static vertical loads as well as for earthquake loads (taking into consideration the accidental torsion effects) using the modal response spectrum analysis, as defined in EC8. The R/C structural elements were designed following the provisions of EC2 (2004) and EC8 (2003). Consequently, a capacity design at frame joints was carried out only along the direction, where the buildings belong to the structural type of frame systems. It should also be noted that the choice of the dimensions of the structural elements' cross-sections, as well as of their reinforcement was made bearing in mind the optimum exploitation of the structural materials strength (steel and concrete). Therefore, the Capacity Ratios CRs (where $CR = \text{Design value of Internal force} / \text{Design strength}$) of all the critical cross-sections due to bending and shear are close to 1.0. The professional program for R/C building analysis and design RAF (2012) was employed in the buildings' design.

Table 2 Common design data for all buildings

Stories' heights H_i	Ductility class	Concrete	Steel	Slab thickness	Slab loads	Masonry loads	Design spectrum (EC8)
3.2 m	Medium (DCM)	C20/25	S500B	3 story	Dead: Perimetric	Masonry loads	Reference
		$E_c=3 \cdot 10^7$	$E_s=2 \cdot 10^8$	buildings:	$G=1.0$	beams:	PGA: $a_{gR}=0.24$ g
		$\nu=0.2$	$\nu=0.3$	7 story	Live: $Q=2.0$	beams:	Importance class: II $\rightarrow \gamma_I=1$
		$w=25$ kN/m^3	$w=78.5$ kN/m^3	16 cm	2.1 kN/m^2	2.1 kN/m^2	Ground type: C

For the modeling of the buildings' nonlinear behavior lumped plasticity (concentrated hinge) models at the column and beam ends, as well as at the base of the walls, were used. The material inelasticity of the structural members was modeled by means of the Modified Takeda hysteresis rule (Otani 1974). It is important to notice that the effects of axial load-biaxial bending moments ($P-M_1-M_2$) interaction at column and wall hinges were taken into consideration by means of the $P-M_1-M_2$ interaction diagram

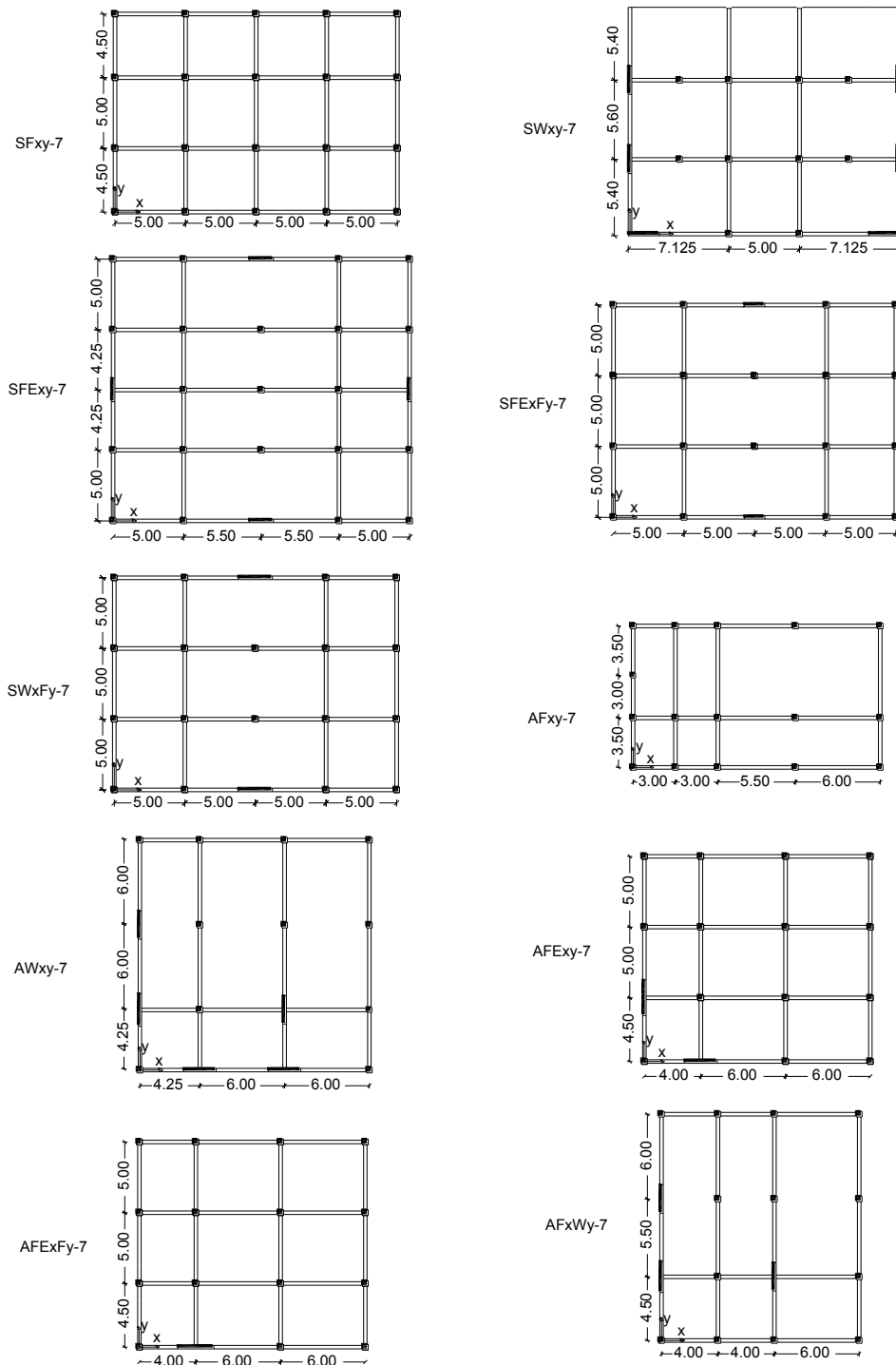


Fig. 2 Plan-views of the selected 7-story buildings

which is implemented in the software used to conduct the analyses (Carr 2004). The yield moments as well as the parameters needed to determine the $P-M_1-M_2$ interaction diagram of the vertical elements' cross sections were determined using appropriate software (XTRACT 2006).

5. Modeling of the masonry infills

Analytical models of masonry infills can be classified

into two categories: the micro- and the macro-models. When the micro-models are used, the behavior of infill walls is represented more accurately, since masonry infills are modeled in detail at components level, such as mortar and bricks. However, such a detailed modeling approach is computationally demanding and, therefore, not suitable for seismic analysis of multibay, multistory structures. On the other hand, the use of macro-models allows representation of the global behavior of masonry infills and their impact on the seismic response of the building. Detailed reviews on

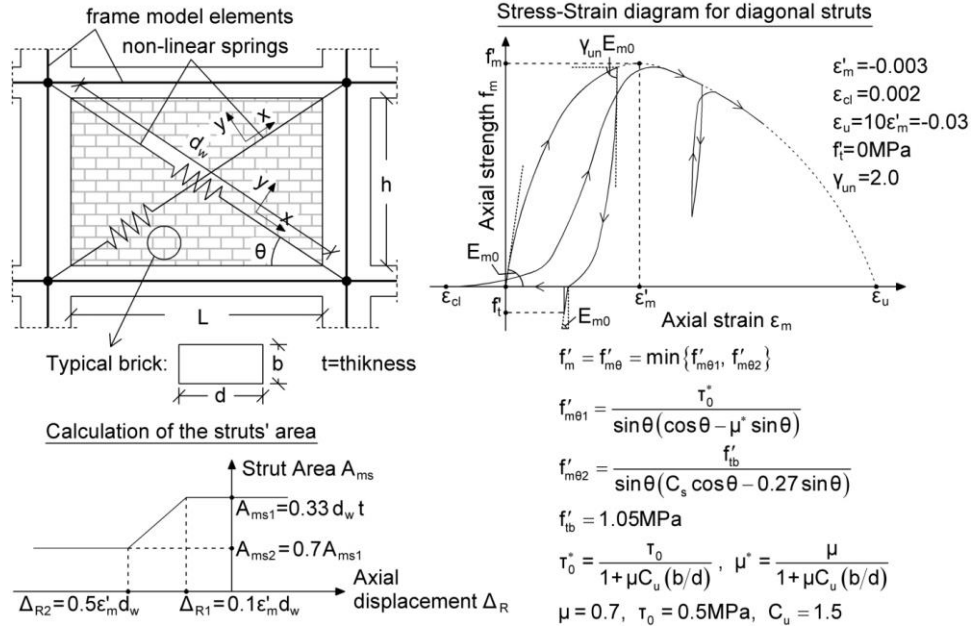


Fig. 3 Simulation of the masonry infill response using the method of diagonal struts

micro- and macro-models of infill walls can be found in (Crisafulli *et al.* 2000, Asteris *et al.* 2011, Tarque *et al.* 2015). According to the second approach, the global effect of masonry infill is represented through single or multiple equivalent diagonal struts. In the present study, the single equivalent diagonal strut model is adopted. Note that this model does not account for the local failure of the node, but it only participates in the global collapse mechanism of the building, which is the main objective of the present research. More specifically, each infill panel was modeled as single equivalent diagonal strut with stress-strain diagram based on the model proposed by Crisafulli (1997), as shown in Fig. 3. In the same figure all the basic parameters used to define the properties of the diagonal struts are presented. It must be noticed that in the present work the values of these parameters were determined based on the code provisions given in EC6 (2005).

6. Analyses procedure

The 60 buildings presented in paragraph 4 were analyzed by Nonlinear Time History Analysis (NTHA) for each one of the 65 earthquake ground motions taking into account the design vertical loads of the structures. The analyses were performed with the aid of the computer program Ruaumoko (2004). Furthermore, as the seismic incident angle with regard to structural axes is unknown, the two horizontal accelerograms of each ground motion were applied along horizontal orthogonal axes forming with the structural axes an angle $\theta = 0^\circ, 5^\circ, 10^\circ, \dots, \dots, 355^\circ$. Thus, for each building and each pair of accelerograms 72 orientations were considered. As a consequence a total of 280,800 NTHA (60 buildings \times 65 earthquake records \times 72 incident angles) were conducted in the present study.

The seismic performance is expressed in the form of the Maximum Interstory Drift Ratio (MIDR), which

corresponds to the maximum drift among the four perimeter frames. The MIDR is considered an effective indicator of global structural and nonstructural damage of R/C buildings (e.g., Gunturi and Shah 1992, Naeim 2001) since it lumps the existing damage of all cross-sections in a single value. So, it has been used in many correlation studies dealing with the estimation of inelastic response of structures (Elenas 2000, Elenas and Meskouris 2001, Liao *et al.* 2001, Yakut and Yilmaz 2008, Masi *et al.* 2011, Kostinakis *et al.* 2015).

Then, in order to evaluate the relative adequacy of ground motion parameters, the correlation between each IM and the MIDR has been computed using the Pearson correlation coefficient (Eq. (3)). The Pearson correlation coefficient, which has been used in several similar correlation studies (Elenas 2000, Elenas and Meskouris 2001, Yakut and Yilmaz 2008), shows how well the data fit a linear relationship and ranges from -1 to 1. The values 1 and -1 indicate that each of the variables is a perfect linear function of the other while 0 shows no linear relationship between the two variables.

$$P_{\text{Pearson}} = \frac{\sum_{i=1}^N (X_i - \bar{X})(Y_i - \bar{Y})}{\sqrt{\sum_{i=1}^N (X_i - \bar{X})^2 \sum_{i=1}^N (Y_i - \bar{Y})^2}} \quad (3)$$

where: \bar{X} and \bar{Y} are the mean values of X_i and Y_i data respectively and N is the number of pairs of values (X_i, Y_i) in the data.

7. Comparative assessment of the results

Fig. 4 illustrates the relationship between PGV and MIDR for the common practice of applying the accelerograms along the structural axes of the building

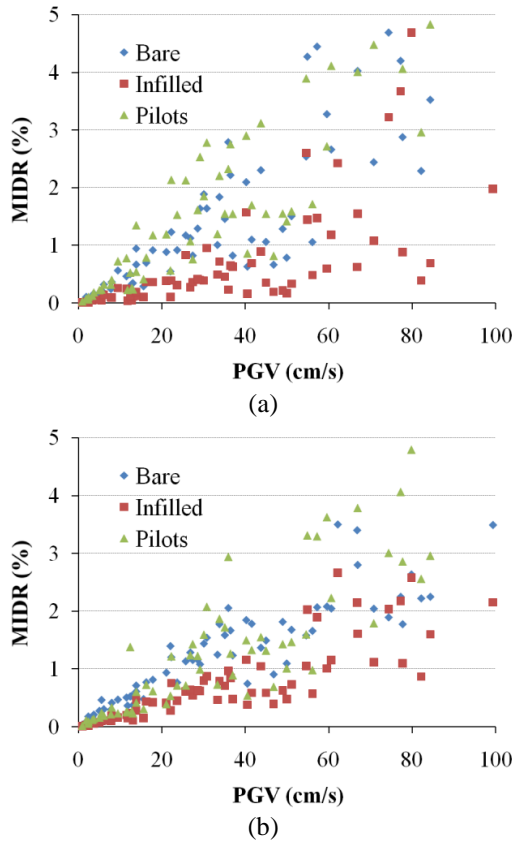


Fig. 4 Relationship between PGV and MIDR ($\theta=0^\circ$) for the 3-story SFxy (a) and the 7-story AFExFy (b)

($\theta=0^\circ$). In particular, the figure presents indicative results for the 3-story building SFxy and for the 7-story building AFExFy. Moreover, note that in the same figure the results concerning the three different assumptions for the distribution of the masonry infills are presented for comparison reasons.

From Fig. 4(a), which depicts the scatter of MIDR for the 3-story building SFxy, we can see that the correlation between the examined IMs and the seismic damage (MIDR) is affected by the distribution of the masonry infills. Note that the correlation is weaker for the infilled building ($p=0.67$) compared with the bare building ($p=0.83$) and the building with pilotis ($p=0.86$). This observation, that the correlation between the IMs and the seismic damage depends on the distribution of the masonry infills, was expected, since the presence of masonry infills may significantly alter the dynamic characteristics of the structure, and consequently modify its seismic performance (e.g., Bertero and Brokken 1983, Ricci *et al.* 2010). Moreover, we can see that the values of MIDR are much smaller for the infilled building, something which is attributed to the fact that the presence of the masonry infills leads to significant increase of the horizontal stiffness, resulting to smaller horizontal displacements. Comparing the results concerning the bare structure and the structure with pilotis, we can see that the values of MIDR are similar. However, it is important to notice that, regarding the structures with pilotis, the analyses showed that, as expected, in most cases the maximum drifts appeared in the

first story, because this was the only story without masonry infills.

From Fig. 4(b) it can be seen that the general conclusions extracted for the 3-story building SFxy are also valid for the 7-story building AFExFy. However, in case of the building AFExFy, the correlation coefficient for the infilled structure seems to attain larger values, which are similar with the corresponding values for the bare structure and the structure with pilotis ($p=0.84$, $p=0.89$ and $p=0.85$ for the infilled structure, the bare structure and the structure with pilotis respectively).

In order to examine the role of the masonry infills on the correlation between the IMs and the seismic damage in case of the common practice of applying the accelerograms along the structural axes of the building ($\theta=0^\circ$), the aggregated results from the Pearson's correlation coefficients concerning both the 3-story and the 7-story buildings are presented in Figs. 5 and 6 respectively. More specifically, the figures illustrate indicative results for the structures SFxy, SFExFy, AFxy and AWxy.

From Figs. 5 and 6 we can see that the correlation between the values of the examined IMs and the MIDR strongly depends on the choice of the ground motion parameter. Note that there are some IMs that lead to small values of correlation coefficients, whereas the use of other IMs produces strong correlation with the seismic damage. In particular, as can be seen from Figs. 5 and 6, the comparative assessment of the seismic IMs evaluated in the present study shows that PGD, d_{ms} and SED led to the poorest correlation with MIDR. This conclusion applies for the most buildings investigated in the present study, irrespective of the special characteristics of the structural system, the number of stories and the presence or not of masonry infills. Concerning the IMs that led to the highest correlation, the analyses results revealed that no certain trend can be found, since it depends on the structural system and the distribution of masonry infills. For example, see that in case of the 7-story infilled building AFxy (Fig. 6(c)), the correlation coefficient when the EDA is used is much larger than the corresponding value produced by SMV. The opposite conclusion is valid for the 7-story infilled building AWxy (Fig. 6(d)), where the value of the Pearson's correlation coefficient is larger when the SMV is adopted as IM. As another example, we can notice that in case of the 3-story infilled building SFxy (Fig. 5(a)), the strongest correlation is observed when I_a is used, something which is not true for the 7-story building with the same structural system (Fig. 6(a)).

A significant conclusion drawn from Figs. 5 and 6 is that, as mentioned above, the degree of correlation between the examined IMs and the MIDR depends on the special characteristics of the structural system, as well as of the number of stories. Note for example that the correlation coefficient when EPA is used for the 7-story infilled building AFxy (Fig. 6(c)) is 0.85, whereas it attains much smaller value ($p=0.68$) in case of the infilled building with structural walls along both horizontal directions (AWxy, Fig. 6(d)). Also, concerning the influence of the number of stories, we can see that in case of the 3-story infilled building AWxy (Fig. 5(d)) the correlation coefficient for EPA attains values around 0.9, whereas the correlation

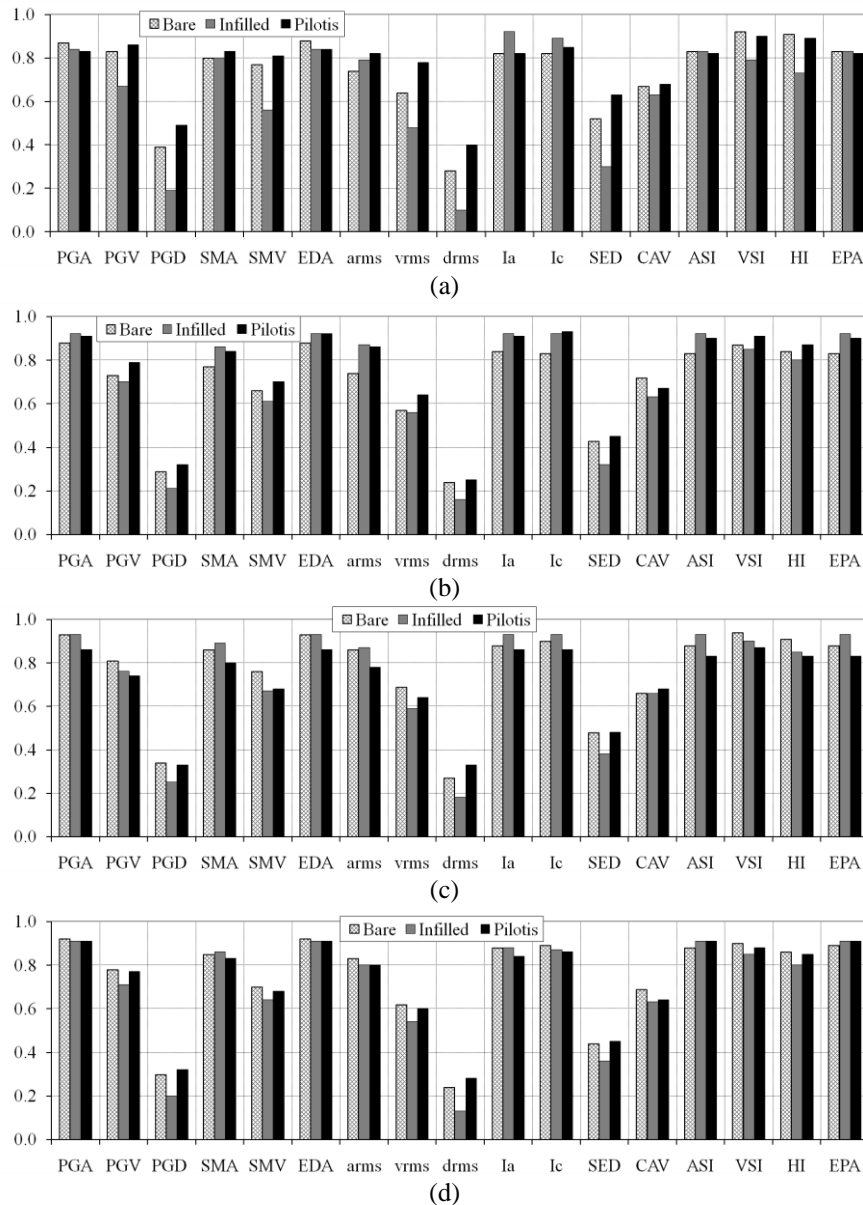


Fig. 5 Pearson's correlation coefficients between seismic intensity measures and MIDR of 3-story buildings for incident angle $\theta=0^\circ$ (SFxy (a), SFExFy (b), AFxy (c) and AWxy (d))

coefficient for the 7-story building with the same structural system (presence of walls along both horizontal directions, Fig. 6(d)) does not exceed the value of 0.7.

Another crucial factor that significantly affects the correlation between the IMs and the seismic damage is the presence or not of the masonry infills, as well as their distribution along the buildings height. For example, Fig. 5(a) indicates that in case of adopting PGV, PGD and SMV the correlation coefficient for the 3-story building SFxy attains much smaller values when the masonry infills are present in all the stories (infilled structure) compared to the bare structure and the structure with pilotis. The way that the masonry infills influence the degree of the correlation between the IMs and MIDR depends on the special characteristics of the structural system and of the choice of the IM. See for example that concerning the 3-story building SFxy (Fig. 5(a)), the correlation between certain

IMs such as I_a and I_c is stronger for the infilled structure. On the contrary, when other IMs, such as PGV, PGD, SMV, v_{rms} , d_{rms} , SED, VSI and HI, are adopted the correlation coefficients for the infilled structure are smaller than the corresponding values for the bare structure and the structure with pilotis. However, the analytical investigation of the results regarding the whole of the examined buildings failed to identify certain trends.

Furthermore, another critical issue that must be examined when estimating the seismic response of 3-dimensional buildings is the influence of the incident angle on the inelastic response. As it has been shown by many researchers, even for quite simple buildings, the angle of seismic incidence can radically alter the analysis results in terms of the elastic response and design of structures (Athanatopoulou 2005, Kostinakis *et al.* 2012), as well as of the inelastic response and damage level, which is expressed

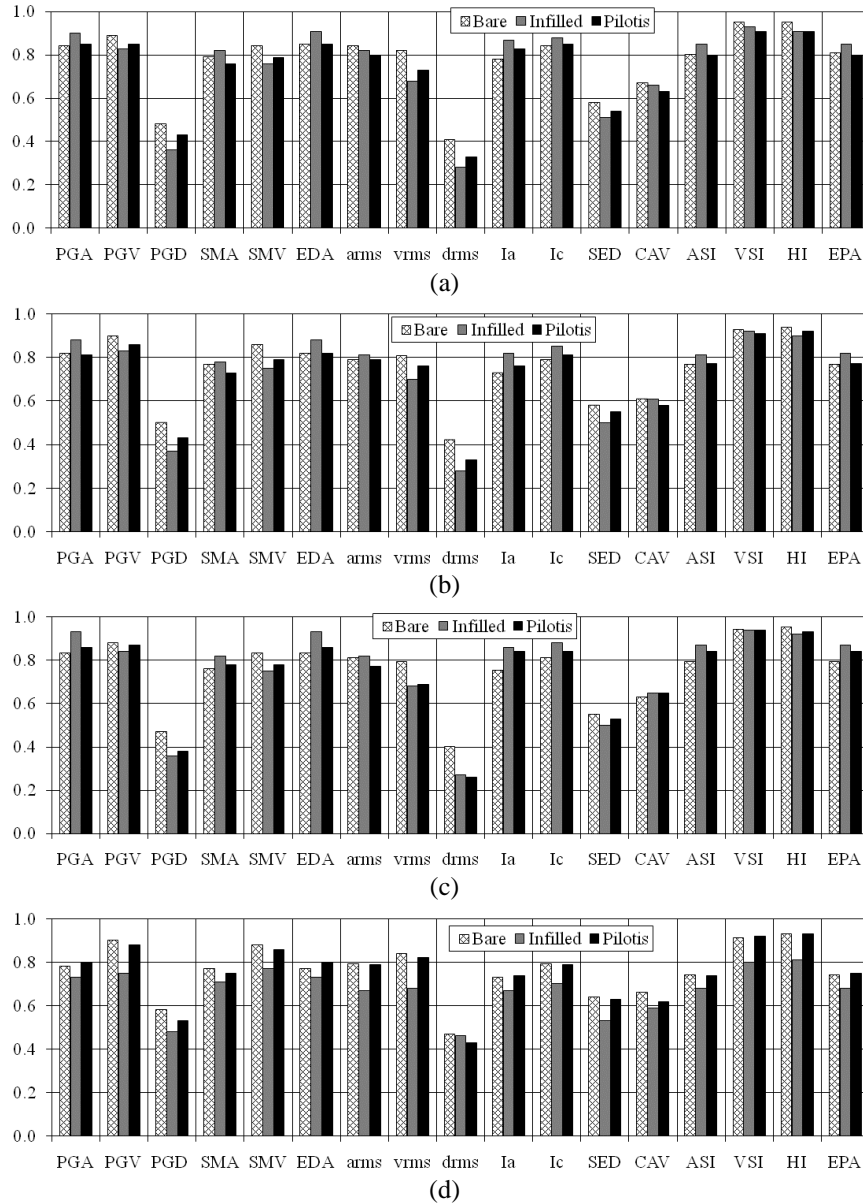


Fig. 6 Pearson's correlation coefficients between seismic intensity measures and MIDR of 7-story buildings for incident angle $\theta=0^\circ$ (SFxy (a), SFExFy (b), AFxy (c) and AWxy (d))

through MIDR in the present study (Rigato and Medina 2007, Lagaros 2010, Lucchini *et al.* 2011, Kostinakis *et al.* 2013, 2015, Fontara *et al.* 2015). As a consequence, we expect that the correlation results will be modified depending on the incident angle. In Fig. 7 indicative results concerning the variation of the Pearson's correlation coefficients between the 17 examined IMs and MIDR with the seismic angle of incidence are presented. The results regard the 7-story bare building SFExFy, the 7-story bare building AFxWy, the 7-story infilled building AFxWy and the 3-story building SFExFy with pilotis.

From this figure we can see that, as was expected, the degree of correlation between the IMs and the seismic damage is affected by the angle of incidence. The influence of the incident angle on the correlation coefficients can be significant depending on the IM, the structural system and the distribution of the masonry infills. For example, see that

regarding the 3-story building SFExFy with pilotis (Fig. 7(d)) the IMs that are mostly affected by the incident angle are d_{rms} , PGD and SED. Also note that for these IMs it seems that the variation of Pearson's correlation coefficient with the angle of incidence is larger for the 3-story building with pilotis (Fig. 7(d)) compared to the corresponding values for the bare 7-story building (Fig. 7(a)). Of significant importance is the fact that the values that the correlation coefficient attains can be highly different for different incident angles, as for example in case of correlation between SED and MIDR of the 3-story building SFExFy (Fig. 7(d)), where the correlation coefficient is 0.62 and 0.38 for angles of incidence $\theta=90^\circ$ and $\theta=220^\circ$ respectively.

In order to examine the influence of the incident angle on the results of the investigation, the maximum value of the MIDR over the 72 incident angles produced by the

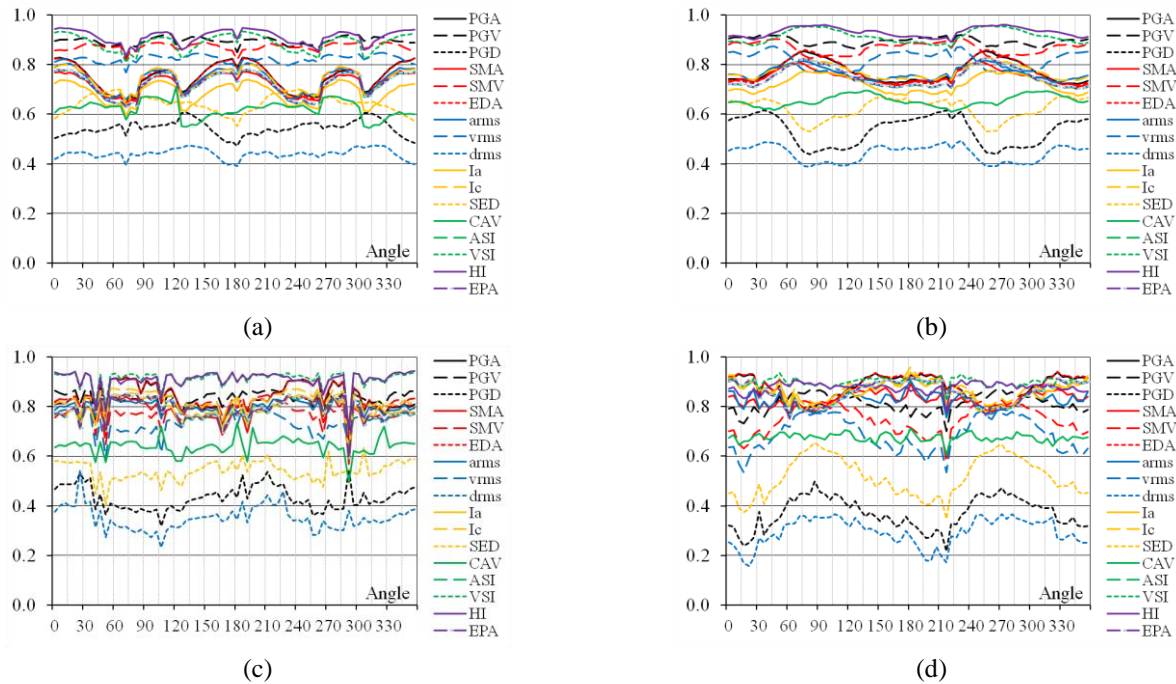


Fig. 7 Variation of Pearson's correlation coefficients between IMs and MIDR with the seismic incident angle (bare 7-story SFExFy (a), bare 7-story AFxWy (b), infilled 7-story AFxWy (c) and 3-story SFExFy with pilotis (d))

ground motions considered in the present study was correlated with the 17 IMs. Fig. 8 presents indicative results regarding the correlation coefficients between MIDR and the seismic IMs for the 3-story building SFxy, the 3-story building SWxy, the 7-story building SFxy and the 7-story building SWxy.

From the above figure, we notice that the general observations made for Figs. 5 and 6 are also valid in case of taking into account the incident angle of the seismic motion. The general conclusion is that, as mentioned above, the degree of correlation between the examined IMs and the MIDR depends on the i) choice of the IM, ii) the special characteristics of the structural system, iii) the number of stories and iv) the presence of masonry infills, as well as their distribution along the height of the building.

With regard to the major aim of the present study, which is the investigation of the impact that the masonry infills have on the correlation between the IMs and the structural damage, we deduce that the influence of the masonry infills is stronger in case of accounting for the angle of incidence that in case of applying the accelerograms along the structural axes ($\theta=0^\circ$). The above conclusion, which is true for the vast majority of the examined buildings, is apparent through comparison of Figs. 5(a) and 8(a), as well as 6(a) and 8(c). The differences between the values of the Pearson's correlation coefficient produced for different distributions of masonry infills can be significant when the maximum MIDR over all angles of incidence is taking into account. See for example that in case of the 7-story building SFxy (Fig. 8(c)) the correlation coefficient between PGA and MIDR attains the values of 0.85, 0.30 and 0.61 for the bare structure, the infilled structure and the structure with pilotis respectively. Also, another general conclusion of great importance, which is valid for the majority of the

investigated buildings in case of accounting for the variable orientation of the seismic motion, is that for the most IMs the correlation is higher for the bare structures, whereas no certain conclusion can be drawn about the comparison between the correlation produced for the infilled structures and the structures with pilotis.

In order to generalize trends, the results for all the considered structural types were ranked to choose the IM with the best global correlation to damage levels. The Figs. 9 (3-story buildings) and 10 (7-story buildings) illustrate the results. In particular, these figures present for each IM the sum of the ranks over the ten different structural systems considered in the study (for more details about the computation of the ranks refer to Masi *et al.* (2011)). The results are presented separately for the common practice of applying the accelerograms along the structural axes ($\theta=0^\circ$), as well as for the case of taking into account the critical incident angle, i.e., the orientation that yields the maximum MIDR. Note that small values of the ranks for a certain IM denote high correlation between the IM and the seismic damage for the most structural types, consequently this IM is more appropriate to be used for the evaluation of seismic performance during the process of the PBEE.

From Fig. 9 it can be deduced that in case of the 3-story buildings the IMs that rank first irrespective of the presence or not of masonry infills are PGA and EDA, whereas the IM that show the poorest correlation results are d_{rms} , PGD, SED, v_{rms} and CAD. Moreover, ASI and EPA provide strong correlation with the seismic damage when the masonry infills are present in all the stories (infilled structures). The above conclusion, however, is not true for the bare structures and the structures with pilotis, for which the ranks of these IMs are larger. The effectiveness of the acceleration related IMs (PGA, EDA, ASI, EPA) as indicators of the seismic

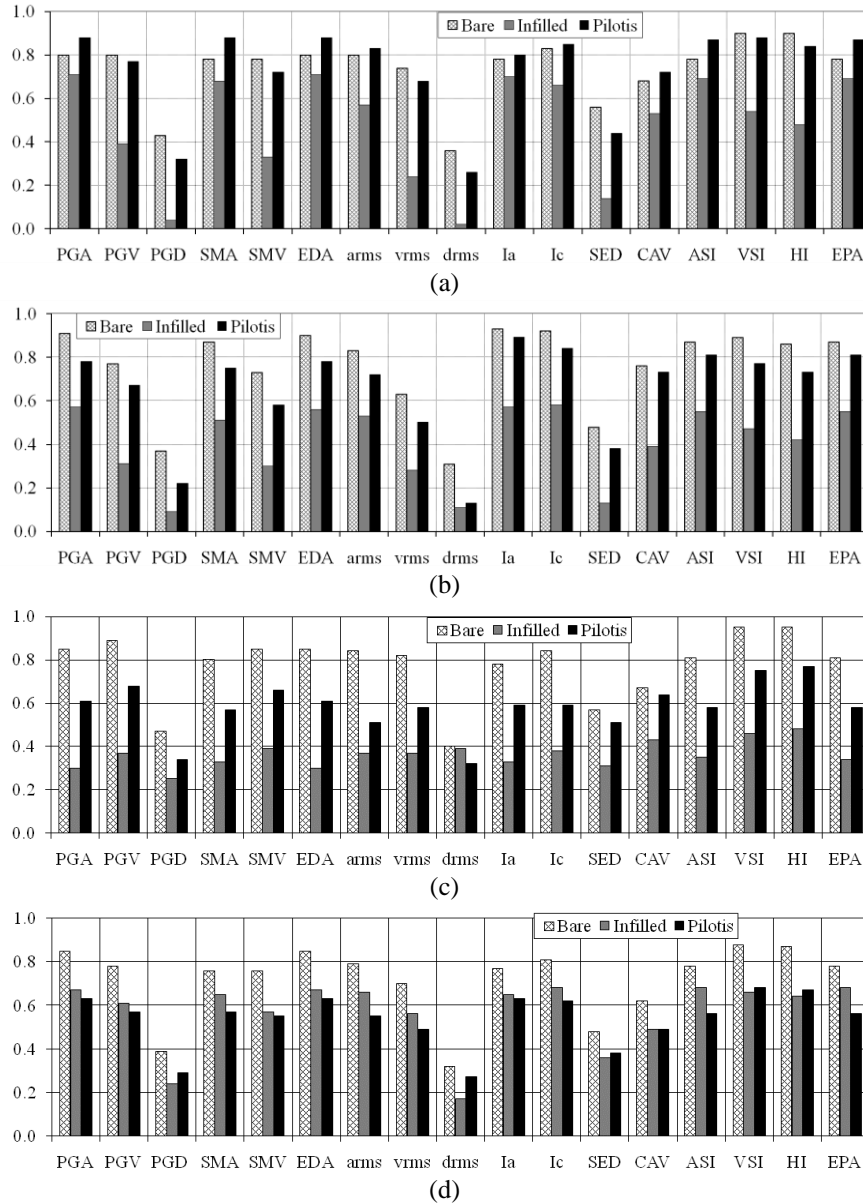


Fig. 8 Pearson's correlation coefficients between seismic intensity measures and maximum MIDR over all incident angles (3-story SFxy (a), 3-story SWxy (b), 7-story SFxy (c), 7-story SWxy (d)).

motion destructiveness is in agreement with previous studies, such as (Riddell 2007). In this study, it has been shown that acceleration related indices are more effective for the short-period structures, which is the case for the 3-story buildings investigated in the present research. Another observation made from Fig. 9 is that VSI leads to high correlation with damage in case of the bare structures. Nevertheless, this IM does not correlate so well with MIDR in case of the structures with pilotis, whereas it provides very poor correlation for the infilled buildings. Furthermore, we can see that I_a , I_c show moderate correlation with MIDR irrespective of the presence of masonry infills. This conclusion is also true when HI is used to be correlated with the MIDR of the bare structures. Of great importance is the fact that all the above conclusions are valid for the common practice of applying the accelerograms along the structural axes ($\theta=0^\circ$), as well

as for the case of taking into account the critical incident angle.

From Fig. 10 it can be seen that in case of the 7-story buildings the IMs that rank first irrespective of the presence or not of masonry infills are VSI and HI, whereas the IM that show the poorest correlation results are d_{rms} , PGD and, SED. The above conclusion agrees with the studies of Riddell (2007) and Kostinakis *et al.* (2015), which revealed that velocity related indices are more effective for the medium-to-long-period structures with fundamental eigenperiod $2.0\text{ s} > T_1 > 0.5\text{ s}$ (7-story buildings). Moreover, CAV leads to small correlation coefficients for the majority of the buildings in the case of $\theta=0^\circ$, as well as in case of the bare structures when the maximum MIDR over all the incident angles is taking into account. Another observation made from Fig. 10 is that PGV leads to high correlation with damage in case of the bare structures. Nevertheless,

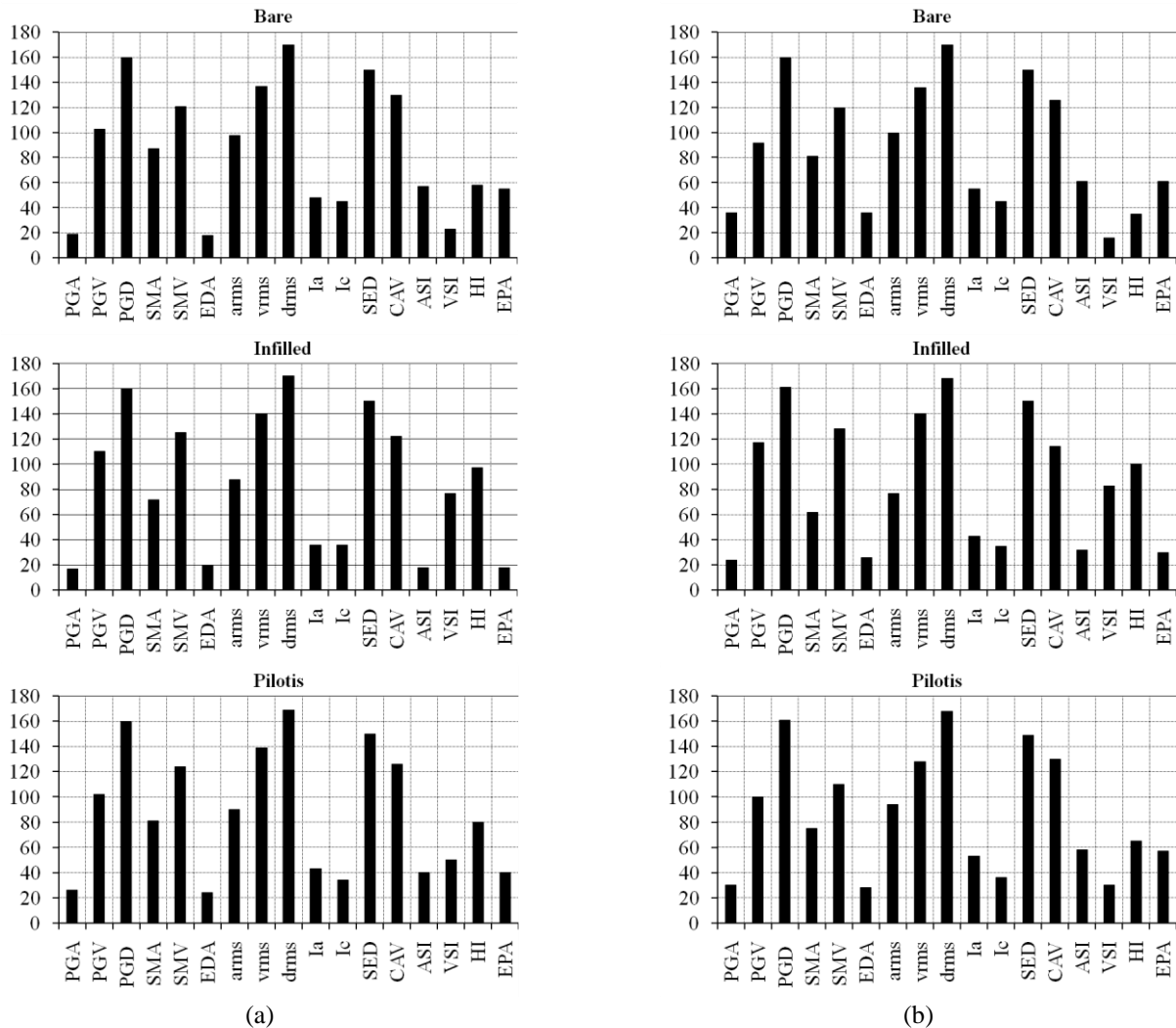


Fig. 9 Sum of the ranks over the ten different structural systems in case of the 3-story buildings for the common practice of applying the accelerograms along the structural axes ($\theta=0^\circ$) (a), as well as for the case of taking into account the critical incident angle (b)

this IM does not correlate so well with MIDR in case of the structures with pilotis, whereas it provides very poor correlation for the infilled buildings. Also, PGA provides strong correlation with the seismic damage when the accelerograms are applied along the structural axes of the infilled buildings. The above conclusion, however, is not true for the bare structures and the structures with pilotis, for which the ranks of this IM are larger. Furthermore, we can see that SMV, a_{rms} , and v_{rms} lead to moderate correlation with damage in case of the bare structures. Yet, the above IMs do not correlate so well with MIDR in case of the infilled structures and the structures with pilotis.

Note that the results of the ranks for the 17 examined IMs presented in the Figs. 9 and 10 concern the ranking of each IM relatively to the others. Consequently, no information is provided about the values of the average correlation coefficients. In the following figures (Figs. 11 and 12) the average values of the Pearson's correlation coefficients between the IMs and MIDR for all the structural types considered in the present study are illustrated. The results are presented separately for the 3-

story (Fig. 11) and the 7-story (Fig. 12) buildings.

From Figs. 11 and 12 we can see that, in general, the conclusions aforementioned when commenting Figs. 5 and 6 are also valid. However, examining the average values of the correlation coefficients some other additional observations can be made. Fig. 11(a) shows that the average correlation coefficient for the 3-story buildings in case of $\theta=0^\circ$ can reach the value of 0.91 for the bare structures (use of PGA and EDA), 0.91 for the infilled structures (use of PGA, EDA, ASI and EPA) and 0.89 for the structures with pilotis (use of PGA, EDA and I_c). Similarly, in case of the 3-story buildings when the critical incident angle is taken into account (Fig. 11(b)), the average value of the correlation coefficient can reach the value of 0.92 for the bare structures (use of VSI), 0.72 for the infilled structures (use of PGA, EDA, ASI and EPA) and 0.84 for the structures with pilotis (use of PGA, EDA, VSI and I_c). Concerning the 7-story buildings, from Fig. 12(a) it is shown that the average correlation coefficient in case of $\theta=0^\circ$ can reach the value of 0.94 for the bare structures (use of HI), 0.91 for the infilled structures (use of VSI) and 0.91

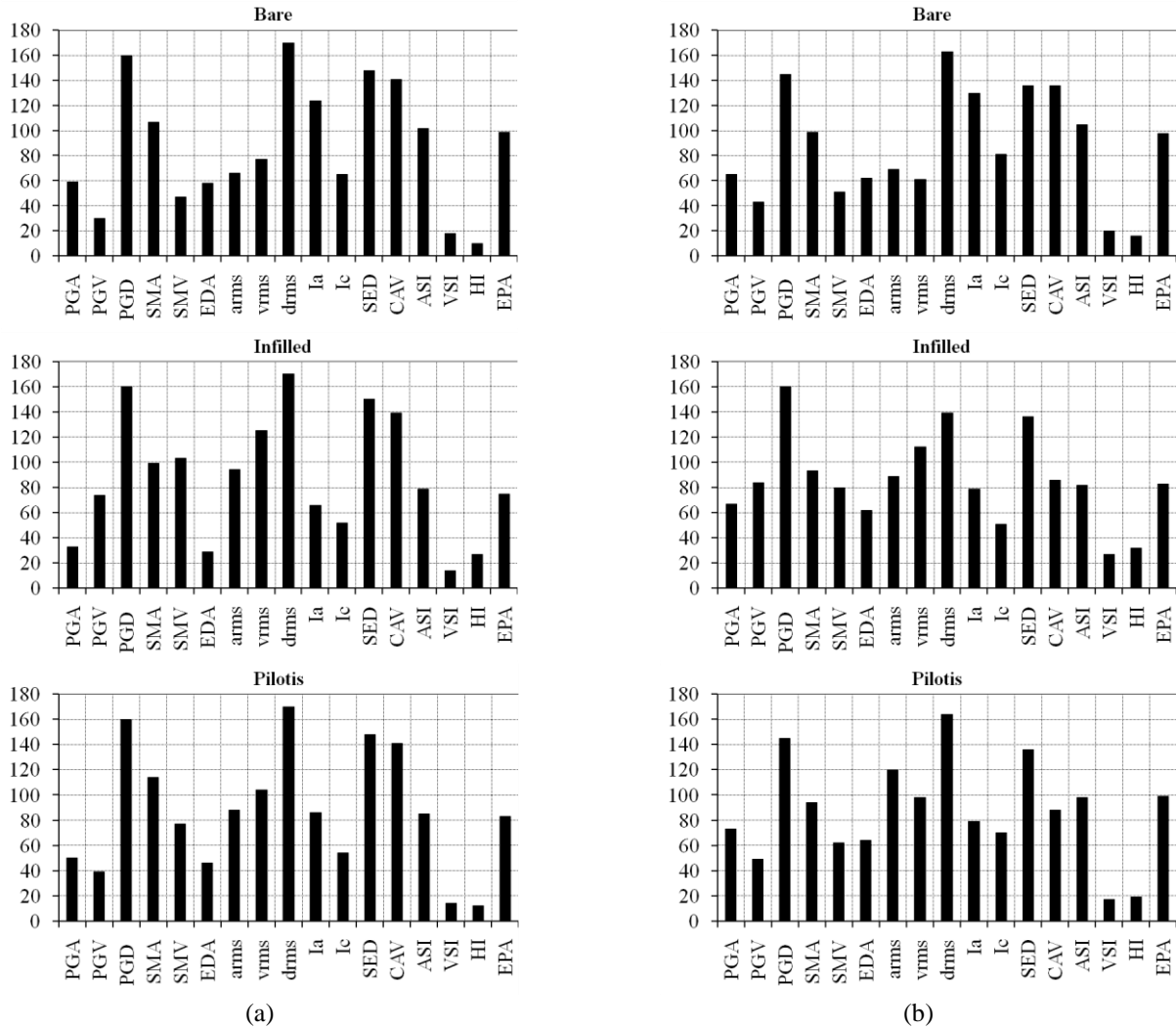


Fig. 10 Sum of the ranks over the ten different structural systems in case of the 7-story buildings for the common practice of applying the accelerograms along the structural axes ($\theta=0^\circ$) (a), as well as for the case of taking into account the critical incident angle (b)

for the structures with pilotis (use of VSI and HI). Similarly, in case of the 7-story buildings when the critical incident angle is taken into account (Fig. 12(b)), the average value of the correlation coefficient can reach the value of 0.92 for the bare structures (use of HI), 0.69 for the infilled structures (use of VSI) and 0.78 for the structures with pilotis (use of HI).

A conclusion of great significance that can be deduced from Figs. 11 and 12 is that the presence or not of masonry infills, as well as their distribution along the building's height strongly influences the correlation between the IMs and the seismic damage in case of using the maximum MIDR over all incident angle. In particular, concerning the 3-story buildings, Fig. 11(b) indicates that the correlation coefficients attain much smaller values for the infilled structures compared to the bare structures and the structures with pilotis. A comparison between the last two masonry distributions reveals that in most cases the correlation is distantly stronger in case of the bare structures. For example, we can see that when SMV is adopted, the average value of Pearson's correlation coefficient is 0.77,

0.44 and 0.71 for the bare structures, the infilled structures and the structures with pilotis respectively. With regard to the 7-story buildings, note that the correlation is much stronger for the bare structures (Fig. 12(b)). A comparison between the infilled structures and the structures with pilotis reveals that in most cases the correlation is higher in case of the structures with pilotis. However, in case of applying the accelerograms along the structural axes the impact of the masonry infills on the correlation is rather weak, so no reliable conclusion can be drawn about the way they influence the correlation coefficients.

8. Conclusions

This paper examines the role of the masonry infills on the correlation between a large number of widely used ground motion intensity measures and the damage state of 3D R/C buildings taking into account the orientation of the seismic input. For the purposes of the above investigation an extensive parametric study is conducted. More

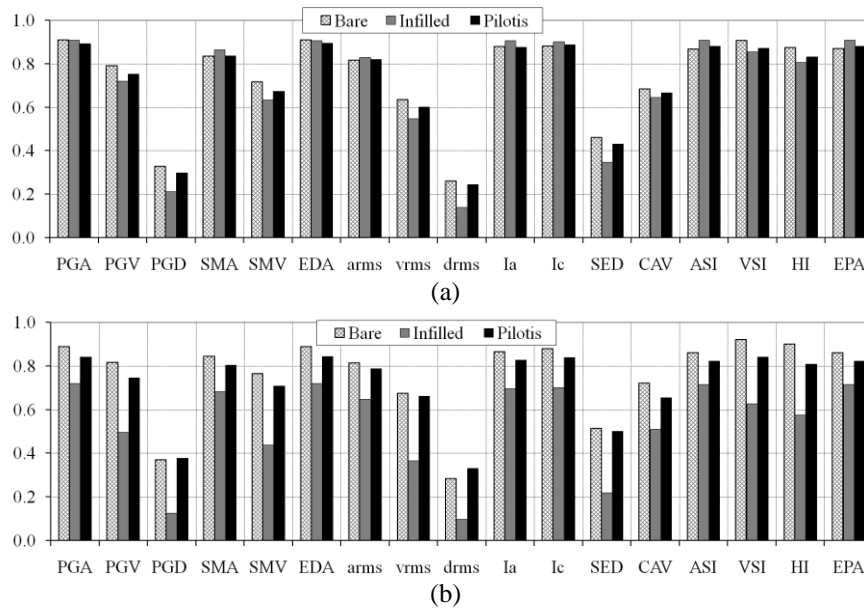


Fig. 11 Pearson's correlation coefficients between seismic intensity measures and MIDR for the 3-story buildings. Average values for all the structural systems (incident angle $\theta=0^\circ$) (a) and maximum MIDR over all incident angles (b)

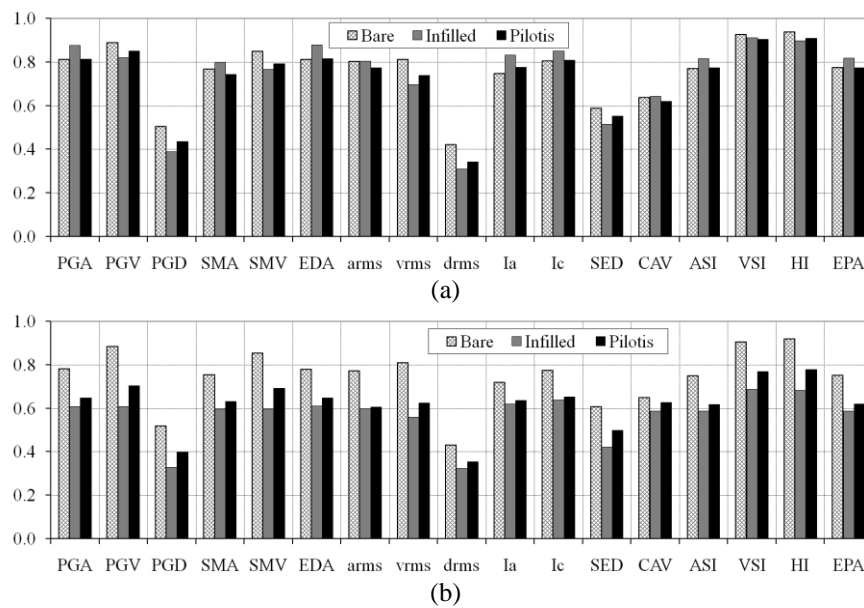


Fig. 12 Pearson's correlation coefficients between seismic intensity measures and MIDR for the 7-story buildings. Average values for all the structural systems (incident angle $\theta=0^\circ$) (a) and maximum MIDR over all incident angles (b)

specifically, 60 3-dimensional R/C buildings with different heights and structural systems are studied. The buildings are classified into three sets regarding the existence or not of masonry infills: the first set contains 20 bare structures, the second set contains 20 structures with masonry infills in all the stories and the third set contains 20 structures with pilotis. The buildings are analyzed by means of Nonlinear Time History Analysis (NTHA) for 65 bidirectional strong motions. In order to account for the influence of the incident angle on the structural response, the two horizontal accelerograms of each ground motion are applied along horizontal orthogonal axes forming an angle $\theta=0^\circ, 5^\circ, 10^\circ, \dots, \dots, 355^\circ$ with the structural axes. For the evaluation of the inelastic structural behavior of each building the

maximum interstory drift ratio is computed. Then, it is correlated with several strong motion intensity measures. The comparative assessment of the results has led to the following conclusions:

- The correlation between the examined IMs and the seismic damage (MIDR) is affected by the distribution of the masonry infills, depending on the choice of the IM, the special characteristics of the structural system and the number of stories.
- In case of the 3-story buildings the IMs that show the highest correlation with seismic damage, irrespective of the presence or not of masonry infills, are PGA and EDA, whereas the IM that show the poorest correlation results are d_{rms} , PGD, SED, v_{rms} and CAD. Moreover,

ASI and EPA provide strong correlation with the seismic damage when the masonry infills are present in all the stories, whereas VSI leads to high correlation with damage in case of the bare structures. Also, HI (for the bare structures), as well as I_a and I_c (for all the three distributions of masonry infills) show moderate correlation with MIDR.

- In case of the 7-story buildings the IMs that show the highest correlation with seismic damage, irrespective of the presence or not of masonry infills, are VSI and HI, whereas the IMs that lead to the poorest correlation results are d_{rms} , PGD and, SED. Moreover, PGV, SMV, a_{rms} , and v_{rms} lead to moderate correlation with damage in case of the bare structures. Also, PGA provides strong correlation with the seismic damage when the accelerograms are applied along the structural axes of the infilled buildings.

- The degree of correlation between the IMs and the seismic damage is affected by the angle of incidence. The influence of the masonry infills' distribution on the correlation coefficients is stronger in case of accounting for the angle of incidence. In this case, the correlation is stronger for the bare structures and weaker for infilled ones. However, in case of applying the accelerograms along the structural axes the impact of the masonry infills on the correlation is rather weak, so no reliable conclusion can be drawn about the way they influence the correlation coefficients.

It must be noted that the aforementioned conclusions are valid for the buildings and ground motions used in the present study. In order to expand them to other structural systems, further investigation is necessary.

Acknowledgments

The author would also like to thank Dr. Konstantinos Morfidis for his help in designing the buildings investigated.

References

- ASCE/SEI 41-06 (2008), Seismic Rehabilitation of Existing Buildings, American Society of Civil Engineers, Reston, VA.
- Asteris, P.G., Antoniou, S.T., Sophianopoulos, D.S. and Chrysostomou, C.Z. (2011), "Mathematical macromodeling of infilled frames: state of the art", *J. Struct. Eng.*, ASCE, **137**(12), 1508-1517.
- Athanatopoulou, A. (2005), "Critical orientation of three correlated seismic components", *Eng. Struct.*, **27**(1), 301-312.
- Bertero, V.V. and Brokken, S. (1983), "Infills in seismic resistant buildings", *J. Struct. Eng.*, ASCE, **109**(6), 1337-1361.
- Beyer, K. and Bommer, J.J. (2006), "Relationships between median values and between aleatory variabilities for different definitions of the horizontal component of motion", *Bull. Seismol. Soc. Am.*, **96**(4A), 1512-1522.
- Cantagallo, C., Camata, G., Spacone, E. and Corotis, R. (2012), "The variability of deformation demand with ground motion intensity", *Prob. Eng. Mech.*, **28**, 59-65.
- Carr, A. (2004), "Ruaumoko-a program for inelastic time-history analysis", *Program Manual*, Department of Civil Engineering, University of Canterbury, New Zealand.
- Cornell, C.A. and Krawinkler, H. (2000), *Progress and Challenges in Seismic Performance Assessment*, PEER Center News.
- Crisafulli, F.J. (1997), "Seismic behaviour of reinforced concrete structures with masonry infills", Ph.D. Thesis, University of Canterbury, Christchurch, New Zealand.
- Crisafulli, F.J., Carr, A.J. and Park, R. (2000), "Analytical modelling of infilled frames structures-a general review", *Bull. NZ Soc. Earthq. Eng.*, **33**(1), 30-47.
- Das, S. and Nau, J.M. (2003), "Seismic design aspects of vertically irregular reinforced concrete buildings", *Earthq. Spectra*, **19**(3), 455-477.
- Dolsek, M. and Fajfar, P. (2008a), "The effect of masonry infills on the seismic response of a four storey reinforced concrete frame-a deterministic assessment", *Eng. Struct.*, **30**, 1991-2001.
- Dolsek, M. and Fajfar, P. (2008b), "The effect of masonry infills on the seismic response of a four storey reinforced concrete frame-a probabilistic assessment", *Eng. Struct.*, **30**, 3186-3192.
- EC2 (2004), Eurocode 2: Design of Concrete Structures, Part 1-1: General Rules and Rules for Buildings, European Committee for Standardization.
- EC6 (2005), Eurocode 6: Design of Masonry Structures - Part 1-1: General Rules for Reinforced and Unreinforced Masonry Structures, European Committee for Standardization.
- EC8 (2003), Eurocode 8: Design of Structures for Earthquake Resistance - Part 1: General Rules, Seismic Actions and Rules for Buildings, European Committee for Standardization.
- EERI (2000), "1999 Kocaeli, Turkey earthquake reconnaissance report", *Earthq. Spectra*, **16**(S1), 237-379.
- Elenas, A. (1997), "Interdependency between seismic acceleration parameters and the behaviour of structures", *Soil. Dyn. Earthq. Eng.*, **16**, 317-322.
- Elenas, A. (2000), "Correlation between seismic acceleration parameters and overall structural damage indices of buildings", *Soil Dyn. Earthq. Eng.*, **20**, 93-100.
- Elenas, A. and Meskouris, K. (2001), "Correlation study between seismic acceleration parameters and damage indices of structure", *Eng. Struct.*, **23**, 698-704.
- European Strong-Motion Database (2003), http://www.isesd.hi.is/ESD_Local/frameset.htm.
- Fontara, I.K.M., Kostinakis, K.G., Manoukas, G.E. and Athanatopoulou, A.M. (2015), "Parameters affecting the seismic response of buildings under bi-directional excitation", *Struct. Eng. Mech.*, **53**(5), 957-979.
- Gunturi, S.K.V. and Shah, H.C. (1992), "Building specific damage estimation", *Proceedings of the 10th World Conference on Earthquake Engineering*, Madrid, Rotterdam, Balkema.
- Imbsen Software Systems (2006), XTRACT: Version 3.0.5, Cross-Sectional Structural Analysis of Components, Sacramento, CA.
- Jayaram, N., Mollaioli, F., Bazzurro, P., De Sortis, A. and Bruno, S. (2010), "Prediction of structural response in reinforced concrete frames subjected to earthquake ground motions", *Proceedings of the US National and 10th Canadian Conference on Earthquake Engineering*, Toronto, Canada, July.
- Kostinakis, K., Athanatopoulou, A. and Avramidis, I. (2012), "Orientation effects of horizontal seismic components on longitudinal reinforcement in R/C Frame elements", *Nat. Hazard. Earth. Syst. Sci.*, **12**, 1-10.
- Kostinakis, K., Athanatopoulou, A. and Avramidis, I. (2013), "Evaluation of inelastic response of 3D single-story R/C frames under bi-directional excitation using different orientation schemes", *Bull. Earthq. Eng.*, **11**, 637-661.
- Kostinakis, K., Athanatopoulou, A. and Morfidis, K. (2015a), "Correlation between ground motion intensity measures and seismic damage of 3D R/C buildings", *Eng. Struct.*, **82**, 151-167.
- Kostinakis, K., Morfidis, K. and Xenidis, H. (2015b), "Damage

- response of multistorey r/c buildings with different structural systems subjected to seismic motion of arbitrary orientation”, *Earthq. Eng. Struct. Dyn.*, **44**, 1919-1937.
- Kramer, S.L. (1996), *Geotechnical Earthquake Engineering*, Prentice-Hall.
- Lagaros, N.D. (2010), “Multicomponent incremental dynamic analysis considering variable incident angle”, *Struct. Infrastr. Eng.*, **6**, 77-94.
- Liao, W.I., Hsiung, C. and Wan, S. (2001), “Earthquake responses of RC moment frames subjected to near-fault ground motions”, *Struct. Des. Tall Build.*, **10**, 219-229.
- Lucchini, A., Monti, G. and Kunnath, S. (2011), “Nonlinear response of two-way asymmetric single-story building under biaxial excitation”, *J. Struct. Eng.*, **137**(1), 34-40.
- Masi, A., Vona, M. and Mucciarelli, M. (2011), “Selection of natural and synthetic accelerograms for seismic vulnerability studies on reinforced concrete frames”, *J. Struct. Eng.*, **137**, 367-378.
- Mondal, G. and Tesfamariam, S. (2014), “Effects of vertical irregularity and thickness of unreinforced masonry infill on the robustness of RC framed buildings”, *Earthq. Eng. Struct. Dyn.*, **43**, 205-223.
- Naeim, F. (2001), *The Seismic Design Handbook*, 1st Edition, Kluwer Academic, Boston, MA.
- Negro, P. and Colombo, A. (1997), “Irregularities induced by nonstructural masonry panels in framed buildings”, *Eng. Struct.*, **19**(7), 576-585.
- Otani, A. (1974), “Inelastic analysis of RC frame structures”, *J. Struct. Div.*, ASCE, **100**(7), 1433-1449.
- Pacific Earthquake Engineering Research Centre (PEER) (2003), Strong Motion Database. <http://peer.berkeley.edu/smcat/>.
- Penzien, J. and Watabe, M. (1975), “Characteristics of 3-D earthquake ground motions”, *Earthq. Eng. Struct. Dyn.*, **3**, 365-373.
- RAF (2012), Structural Analysis and Design Software v.3.3.2. TOL (Engineering Software House), Iraklion, Crete, Greece.
- Ricci, P., De Luca, F. and Verderame, G.M. (2010), “6th April 2009 L’Aquila earthquake, Italy: reinforced concrete building performance”, *Bull. Earthq. Eng.*, **9**(1), 285-305.
- Ricci, P., De Ricci, M.T., Verderame, G.M. and Manfredi, G. (2013), “Influence of infill distribution and design typology on seismic performance of low-and mid-rise RC buildings”, *Bull. Earthq. Eng.*, **11**, 1585-1616.
- Ricci, P., Verderame, G.M. and Manfredi, G. (2011), “Analytical investigation of elastic period of infilled RC MRF buildings”, *Eng. Struct.*, **33**, 308-319.
- Riddell, R. (2007), “On ground motion intensity indices”, *Earthq. Spectra*, **23**, 147-173.
- Rigato, A. and Medina, R. (2007), “Influence of angle of incidence on seismic demands for inelastic single-storey structures subjected to bi-directional ground motions”, *Eng. Struct.*, **29**, 2593-2601.
- Tarque, N., Candido, L., Camata, G. and Spacone, E. (2015), “Masonry infilled frame structures: state-of-the-art review of numerical modelling”, *Earthq. Struct.*, **8**(3), 733-759.
- Yakut, A. and Yilmaz, H. (2008), “Correlation of deformation demands with ground motion intensity”, *J. Struct. Eng.*, **134**(12), 1818-1828.
- Yuen, Y.P. and Kuang, J.S. (2015), “Nonlinear seismic response and lateral force transfer mechanisms of RC frames with different infill configurations”, *Eng. Struct.*, **91**, 125-140.